

Highly Luminescent Cu(I)–Phenanthroline Complexes in Rigid Matrix and Temperature Dependence of the Photophysical Properties

Delphine Felder,[‡] Jean-François Nierengarten,^{*,‡} Francesco Barigelletti,^{*,†} Barbara Ventura,[†] and Nicola Armaroli^{*,†}

Contribution from Institut de Physique et Chimie des Matériaux de Strasbourg, Groupe des Matériaux Organiques, Université Louis Pasteur et CNRS, 23 rue du Loess, 67037 Strasbourg, France, and Istituto di Fotochimica e Radiazioni d'Alta Energia del CNR, via P. Gobetti 101, 40129 Bologna, Italy

Received December 27, 2000

Abstract: We synthesized new $[\text{Cu}(\text{NN})_2]^+$ -type complexes where NN = **2–5** and denotes a 2,9-disubstituted-1,10-phenanthroline ligand (related complexes of **1** and **6** ligands are used for reference purposes). For **2**, **3**, and **4** the ligand substituents are long alkyl-type fragments, whereas in **5** a phenyl ring is directly attached to the chelating unit. At 298 K the four complexes display relatively intense metal-to-ligand-charge-transfer (MLCT) emission bands with maxima around 720 nm, $\Phi_{\text{em}} \approx 1 \times 10^{-3}$ and $\tau > 100$ ns in deaerated CH_2Cl_2 . The emission behavior at 77 K in a $\text{CH}_2\text{Cl}_2/\text{MeOH}$ matrix is quite different for complexes of alkyl- (**2–4**) versus phenyl-substituted (**5**) ligands. The former exhibit very intense emission bands centered around 642 nm and hypsochromically shifted with respect to 298 K, whereas the luminescence band of $[\text{Cu}(\mathbf{5})_2]^+$ is faint and shifted toward the infrared side. These results prompted us to study in detail the temperature dependence of luminescence properties of $[\text{Cu}(\mathbf{2})_2]^+$ and $[\text{Cu}(\mathbf{5})_2]^+$ in the 300–96 K range. For both complexes the excited state lifetimes increase monotonically by decreasing temperatures, and the trend is well described by an Arrhenius-type treatment involving two equilibrated MLCT excited levels. The emission bands show a similar behavior for the two compounds (intensity decrease and red-shift) only in the 300–120 K range, when the solvent is fluid. In the frozen regime ($T \leq 120$ K), the emission intensity of $[\text{Cu}(\mathbf{5})_2]^+$ continues to drop, whereas that of $[\text{Cu}(\mathbf{2})_2]^+$ exhibits a dramatic intensity increase. We interpret this different behavior in terms of structural factors, suggesting that long alkyl-chains in the 2,9-phenanthroline positions are optimal to prevent significant ground- and excited-state distortions in rigid matrix. We show that our results do not contradict current models describing the photophysics of $[\text{Cu}(\text{NN})_2]^+$ but, instead, bring further evidence to support their validity. They also suggest guidelines for the design of Cu(I)–phenanthroline complexes showing optimized luminescence performances both in fluid and in rigid matrix, an elusive goal for over two decades.

Introduction

The investigation of the luminescence properties of bisphenanthroline complexes of copper(I), herein abbreviated $[\text{Cu}(\text{NN})_2]^+$, has been the focus of many research reports that have been recently reviewed.^{1–3} The underlying motivation for this type of study has to do with possible practical applications, for instance in the field of energy conversion and storage.^{4–7} In the area of inorganic photochemistry other metal complexes, for instance those of the ruthenium(II)–polypyridine family,⁸ have attracted a great deal of attention since they proved to be very useful for the design of excitation energy transduction schemes and storage^{9–11} or for the development of various

sensing abilities based on luminescence.¹² In general, in view of practical uses, some requirements related to the capability of light absorption and formation of excited states should be met.¹³ Indeed, while several Cu(I)–phenanthrolines with strong absorption in the visible spectral region (vis) have been prepared,^{1,2} long-lived ($\tau > 100$ ns) and luminescent excited states have not been always observed. Reasons have mainly to do with the fact that in $[\text{Cu}(\text{NN})_2]^+$ -type complexes, the lowest-lying excited levels are of metal-to-ligand-charge-transfer (MLCT) nature¹⁴ and their formation is accompanied by extended structural rearrangements.³ These can be described in terms of a release of the ground-state pseudotetrahedral geometry (D_{2d}), to a more open geometry, mainly occurring via “flattening” and “rocking” distortions.¹⁵ In this way, the thermally equilibrated MLCT excited states¹⁶ undergo a con-

[‡] IPCMS, Strasbourg.

[†] Istituto FRAE/CNR, Bologna. E-mail: armaroli@frae.bo.cnr.it. Fax +39-051-6399844.

(1) Armaroli, N. *Chem. Soc. Rev.* **2001**, *30*, 113.

(2) Scaltrito, D. V.; Thompson, D. W.; O'Callaghan, J. A.; Meyer, G. J. *Coord. Chem. Rev.* **2000**, *208*, 243.

(3) McMillin, D. R.; McNett, K. M. *Chem. Rev.* **1998**, *98*, 1201.

(4) Bignozzi, C. A.; Argazzi, R.; Kleverlaan, C. J. *Chem. Soc. Rev.* **2000**, *29*, 87.

(5) Schwab, P. F. H.; Levin, M. D.; Michl, J. *Chem. Rev.* **1999**, *99*, 1863.

(6) Balzani, V.; Campagna, S.; Dentì, G.; Juris, A.; Serroni, S.; Venturi, M. *Acc. Chem. Res.* **1998**, *31*, 26.

(7) Breddels, P. A.; Berdowski, P. A. M.; Blasse, G. *Recl. Trav. Chim. Pays-Bas* **1981**, *100*, 439.

(8) Juris, A.; Balzani, V.; Barigelletti, F.; Campagna, S.; Belsler, P.; von Zelewsky, A. *Coord. Chem. Rev.* **1988**, *84*, 85.

(9) Barigelletti, F.; Flamigni, L. *Chem. Soc. Rev.* **2000**, *29*, 1.

(10) Harriman, A.; Ziesse, R. *Chem. Commun.* **1996**, 1707.

(11) Balzani, V.; Juris, A.; Venturi, M.; Campagna, S.; Serroni, S. *Chem. Rev.* **1996**, *96*, 759.

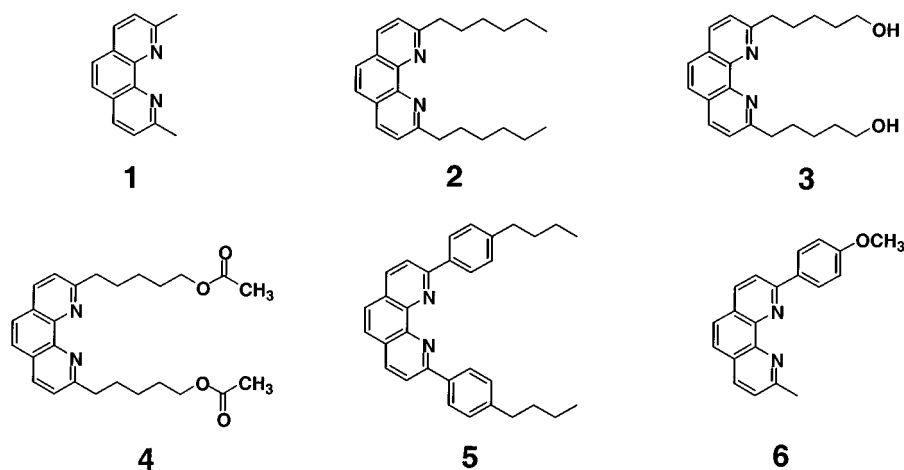
(12) For a series of papers on luminescent chemical sensors based on transition metal complexes, see: *Coord. Chem. Rev.* **2000**, *Vol. 205*.

(13) Roundhill, D. M. *Photochemistry and Photophysics of Metal Complexes*; Plenum Press: New York, 1994.

(14) McMillin, D. R.; Buckner, M. T.; Ahn, B. T. *Inorg. Chem.* **1977**, *16*, 943.

(15) Dobson, J. F.; Green, B. E.; Healy, P. C.; Kennard, C. H. L.; Pakawatchai, C.; White, A. H. *Aust. J. Chem.* **1984**, *37*, 649.

Chart 1



sistent energetic stabilization, which is facilitated by an easy access of the donating solvent toward the formally d^9 Cu(II) center.¹⁷ Relevant consequences, nowadays well documented by the investigations of McMillin,^{3,18–25} Karpishin,^{26–29} G. J. Meyer,^{2,30–32} and others,^{33–38} are related to the fact that deactivation of the excited level is subject to strongly enhanced nonradiative paths via effects concerned with the “energy-gap law”^{39–41} or even with direct quenching by solvent molecules.¹⁷

(16) Everly, R. M.; McMillin, D. R. *J. Phys. Chem.* **1991**, *95*, 9071.

(17) Everly, R. M.; McMillin, D. R. *Photochem. Photobiol.* **1989**, *50*, 711.

(18) Buckner, M. T.; McMillin, D. R. *J. Chem. Soc., Chem. Commun.* **1978**, 759.

(19) Kirchhoff, J. R.; Gamache, R. E.; Blaskie, M. W.; Del Paggio, A. A.; Lengel, R. K.; McMillin, D. R. *Inorg. Chem.* **1983**, *22*, 2380.

(20) Phifer, C. C.; McMillin, D. R. *Inorg. Chem.* **1986**, *25*, 1329.

(21) Ichinaga, A. K.; Kirchhoff, J. R.; McMillin, D. R.; Dietrich-buecker, C. O.; Marnot, P. A.; Sauvage, J. P. *Inorg. Chem.* **1987**, *26*, 4290.

(22) Gushurst, A. K. I.; McMillin, D. R.; Dietrich-Buecker, C. O.; Sauvage, J. P. *Inorg. Chem.* **1989**, *28*, 4070.

(23) Eggleston, M. K.; McMillin, D. R.; Koenig, K. S.; Pallenberg, A. *J. Inorg. Chem.* **1997**, *36*, 172.

(24) Cunningham, C. T.; Cunningham, K. L. H.; Michalec, J. F.; McMillin, D. R. *Inorg. Chem.* **1999**, *38*, 4388.

(25) Cunningham, C. T.; Moore, J. J.; Cunningham, K. L. H.; Fanwick, P. E.; McMillin, D. R. *Inorg. Chem.* **2000**, *39*, 3638.

(26) Miller, M. T.; Gantzel, P. K.; Karpishin, T. B. *Angew. Chem., Int. Ed.* **1998**, *37*, 1556.

(27) Miller, M. T.; Karpishin, T. B. *Inorg. Chem.* **1999**, *38*, 5246.

(28) Miller, M. T.; Gantzel, P. K.; Karpishin, T. B. *Inorg. Chem.* **1999**, *38*, 3414.

(29) Miller, M. T.; Gantzel, P. K.; Karpishin, T. B. *J. Am. Chem. Soc.* **1999**, *121*, 4292.

(30) Castellano, F. N.; Ruthkosky, M.; Meyer, G. J. *Inorg. Chem.* **1995**, *34*, 3.

(31) Ruthkosky, M.; Kelly, C. A.; Zaros, M. C.; Meyer, G. J. *J. Am. Chem. Soc.* **1997**, *119*, 12004.

(32) Ruthkosky, M.; Kelly, C. A.; Castellano, F. N.; Meyer, G. J. *Coord. Chem. Rev.* **1998**, *171*, 309.

(33) Vögtle, F.; Lüer, I.; Balzani, V.; Armaroli, N. *Angew. Chem., Int. Ed. Engl.* **1991**, *30*, 1333.

(34) Dietrich-Buecker, C. O.; Nierengarten, J. F.; Sauvage, J. P.; Armaroli, N.; Balzani, V.; De Cola, L. *J. Am. Chem. Soc.* **1993**, *115*, 11237.

(35) Armaroli, N.; Balzani, V.; Barigelletti, F.; De Cola, L.; Flamigni, L.; Sauvage, J. P.; Hemmert, C. *J. Am. Chem. Soc.* **1994**, *116*, 5211.

(36) Dietrich-Buecker, C. O.; Sauvage, J. P.; Armaroli, N.; Ceroni, P.; Balzani, V. *Angew. Chem., Int. Ed. Engl.* **1996**, *35*, 1119.

(37) Armaroli, N.; Diederich, F.; Dietrich-Buecker, C. O.; Flamigni, L.; Marconi, G.; Nierengarten, J. F.; Sauvage, J. P. *Chem.—Eur. J.* **1998**, *4*, 406.

(38) Armaroli, N.; Boudon, C.; Felder, D.; Gisselbrecht, J. P.; Gross, M.; Marconi, G.; Nicoud, J. F.; Nierengarten, J. F.; Vicinelli, V. *Angew. Chem., Int. Ed.* **1999**, *38*, 3730.

(39) Caspar, J. V.; Kober, E. M.; Sullivan, B. P.; Meyer, T. J. *J. Am. Chem. Soc.* **1982**, *104*, 630.

(40) Englman, R.; Jortner, J. *J. Mol. Phys.* **1970**, *18*, 145.

The strongly appealing possibility of using cheap copper(I) complexes for replacing the more expensive compounds based on ruthenium(II) or other metal ions, along with the need for a deeper understanding of the correlation between structural processes and photophysical properties, have pushed a continuous progress in the design of photoluminescent $[\text{Cu}(\text{NN})_2]^+$ complexes.¹ In these, a common motif has been that of using appended units to the phenanthroline frame so as to block as much as possible the excited-state distortions. Nowadays, complexes are available that feature remarkable luminescence properties. For instance, $[\text{Cu}(\text{dbtmp})_2]^+$ exhibits $\tau = 920$ ns and $\phi = 0.0062$ in degassed CH_2Cl_2 (dbtmp = 2,9-dibutyl-1,10-phenanthroline).²⁴ Here, steric effects exerted by *n*-butyl groups appended at 2,9 and buttressing methyl groups at 3, 4, 7, and 8 phenanthroline positions cooperate to effectively block the excited state close to the ground-state geometry. A highly emissive compound where blocking of the geometry was also successfully obtained is the heteroleptic $[\text{Cu}(\text{dbp})(\text{dmp})]^+$ complex where $\tau = 730$ ns and $\phi = 0.01$ in degassed CH_2Cl_2 (dbp = 2,9-di-*tert*-butyl-1,10-phenanthroline, dmp = 2,9-dimethyl-1,10-phenanthroline).²⁹ A further approach for blocking structural rearrangements at the excited state has been based on the use of aryl groups appended to the phen unit.²² In this case, one exploits interligand π -stacking interactions (involving the aryl group of one ligand and a ring of the opposite ligand) which cause deviations from the D_{2d} symmetry already for the ground state. Remarkably, upon light absorption the excited-state rearrangement is somewhat restrained as an effect of this type of interactions.

In line with the above-mentioned approaches, we have prepared the $[\text{Cu}(\text{NN})_2]^+$ complexes of the ligands 1–5 illustrated in Chart 1, and we have then studied their photophysical properties in detail. In some of these compounds the basic photoactive $[\text{Cu}(\text{phen})_2]^+$ unit is equipped with alkyl chains that might be long enough to wrap it. We have thus observed good luminescence properties at room temperature, as a consequence of geometric effects leading to protection of the cation center from interactions with the environment.¹⁷ Both alkyl- ($[\text{Cu}(\mathbf{2})_2]^+$, $[\text{Cu}(\mathbf{3})_2]^+$, $[\text{Cu}(\mathbf{4})_2]^+$) and aryl-phenanthroline ($[\text{Cu}(\mathbf{5})_2]^+$) cases have been worked out. The complexes $[\text{Cu}(\mathbf{1})_2]^{+1}$ and $[\text{Cu}(\mathbf{6})_2]^+$,³⁴ have been employed for reference purposes. On the basis of the well-known two-level model for the lowest MLCT excited states of $[\text{Cu}(\text{NN})_2]^+$ (vide infra),^{16,19} a detailed investigation of the temperature dependence of the luminescence for two representative cases, $[\text{Cu}(\mathbf{2})_2]^+$ and $[\text{Cu}(\mathbf{5})_2]^+$, has been

(41) Freed, K.; Jortner, J. *J. Chem. Phys.* **1970**, *52*, 6272.

carried out in the 300–96 K range. We have found that the change of the luminescence properties (intensity and lifetime) across the glass-to-fluid transition region of the solvent^{42,43} provides useful hints for understanding the role of the structural and electronic factors that affect the excited levels of $[\text{Cu}(\text{NN})_2]^+$ complexes. Importantly, for the first time, it is reported that in some cases (i.e., complexes with long alkyl residues on the phenanthroline ligands) the luminescence intensity pattern is oscillating as a function of temperature: a decrease is found in the range 300–120 K, then a dramatic increase is recorded by further cooling. This yields strongly luminescent $[\text{Cu}(\text{NN})_2]^+$ complexes below 100 K, quite rarely observed earlier.⁴⁴

Experimental Section

General Synthetic Procedure. Reagents and solvents were purchased as reagent grade and used without further purification. Commercially available 1,10-phenanthroline monohydrate was dried by three successive azeotropic distillation in toluene/ethanol (51:35). Compounds **3**⁴⁵ and $(\text{I})_2\text{Cu}\cdot\text{BF}_4$ ¹⁴ were prepared according to the literature. All reactions were performed in standard glassware under an inert Ar atmosphere. Evaporation and concentration were done at water aspirator pressure and drying in vacuo at 10^{-2} Torr. Thin layer chromatography (TLC) was performed on glass sheets coated with silica gel 60 F₂₅₄ purchased from E. Merck, visualization by UV light. Melting points were measured on an electrothermal digital melting point apparatus and are uncorrected. IR spectra (cm^{-1}) were measured on an ATI Mattson Genesis Series FTIR instrument. NMR spectra were recorded on a Bruker AC 200 (200 MHz) with solvent peaks as reference. Elemental analysis were performed by the analytical service at the Institut Charles Sadron (Strasbourg, France).

Preparation of Di-2,9-hexyl-1,10-phenanthroline (2). A 2.5 M *n*-hexyllithium solution (10 mL, 25 mmol) was added by syringe to an argon-flushed, stirred suspension of 1,10-phenanthroline (2.0 g, 10.09 mmol) in dry Et₂O (100 mL) at room temperature. The resulting dark red mixture was stirred for 48 h and then hydrolyzed with water. The bright yellow ether layer was decanted and the aqueous layer extracted with CH₂Cl₂ (3×). The combined organic layers were thereafter rearomatized by addition of MnO₂ (30 g), dried (MgSO₄), and filtered; the filtrate was then evaporated to dryness. Column chromatography on SiO₂ (CH₂Cl₂/hexane 5:1) yielded **2** as a colorless glassy product (2.47 g, 70%). ¹H NMR (CDCl₃, 200 MHz): δ = 0.91 (t, *J* = 6 Hz, 6H), 1.30–1.60 (m, 12H), 1.92 (m, 4H), 3.22 (t, *J* = 6 Hz, 4H), 7.53 (d, *J* = 8 Hz, 2H), 7.72 (s, 2H), 8.16 (d, *J* = 8 Hz, 2H); ¹³C NMR (CDCl₃, 50 MHz): δ = 13.95, 22.45, 29.34, 29.57, 31.64, 39.37, 122.12, 125.23, 126.85, 135.96, 145.24, 163.05; C₂₄H₃₂N₂ (348.53): calcd C 82.71, H 9.25, N 8.04; found C 82.70, H 9.31, N 7.90.

Preparation of Di-2,9-(5-acetyloxypropyl)-1,10-phenanthroline (4). A solution of pyridine (0.25 mL, 3.12 mmol) and DMAP (87 mg, 0.70 mmol) in CH₂Cl₂ (50 mL) was added dropwise at room temperature to an argon-flushed, stirred solution of **3** (500 mg, 1.41 mmol) and acetyl chloride (0.222 mL, 3.12 mmol). After 4 h, the resulting solution was washed with water, dried (MgSO₄), filtered, and evaporated to dryness. Column chromatography on SiO₂ (CH₂Cl₂/5% MeOH) yielded **4** as a colorless glassy product (330 mg, 0.76 mmol, 53%). ¹H NMR (CDCl₃, 200 MHz): δ = 1.56 (m, 8H), 1.92 (m, 4H), 2.05 (s, 6H), 3.22 (t, *J* = 6 Hz, 4H), 4.10 (t, *J* = 6 Hz, 4H), 7.51 (d, *J* = 8 Hz, 2H), 7.71 (s, 2H), 8.15 (d, *J* = 8 Hz, 2H); ¹³C NMR (CDCl₃, 50 MHz): δ = 21.01, 26.06, 28.52, 29.31, 39.30, 64.48, 122.32, 125.51, 127.11, 136.26, 145.01, 162.33, 171.83; IR (CH₂Cl₂): 1731 cm^{-1} (C=O); C₂₆H₃₂O₄N₂·H₂O (454.57): calcd C 68.70, H 7.54; found C 68.39, H 7.24.

(42) Barigelletti, F.; Belsler, P.; von Zelewsky, A.; Juris, A.; Balzani, V. *J. Phys. Chem.* **1985**, *89*, 3680.

(43) Barigelletti, F.; Juris, A.; Balzani, V.; Belsler, P.; von Zelewsky, A. *J. Phys. Chem.* **1987**, *91*, 1095.

(44) Everly, R. M.; Ziessel, R.; Suffert, J.; McMillin, D. R. *Inorg. Chem.* **1991**, *30*, 559.

(45) Nierengarten, J. F.; Dietrich-Buchecker, C. O.; Sauvage, J. P. *New J. Chem.* **1996**, *20*, 685.

Preparation of 2-(4-*n*-Butylphenyl)-1,10-phenanthroline. A 1.6 M *n*-BuLi solution (6.9 mL, 11.04 mmol) was added by syringe at room temperature to an argon-flushed, stirred solution of 4-bromo-*n*-butylbenzene (2.34 g, 11.00 mmol) in dry Et₂O (40 mL). After 1.5 h, the resulting yellow solution was added under argon to a degassed suspension of 1,10-phenanthroline (2.0 g, 10.09 mmol) in dry Et₂O (100 mL) cooled to 0 °C (ice–water bath). The resulting dark red mixture was stirred for 5 h and then hydrolyzed with water. The bright yellow ether layer was decanted and the aqueous layer extracted with CH₂Cl₂ (3×). The combined organic layers were thereafter rearomatized by addition of MnO₂ (30 g), dried (MgSO₄), and filtered; the filtrate was then evaporated to dryness. Column chromatography on SiO₂ (CH₂Cl₂) yielded 2-(4-*n*-butylphenyl)-1,10-phenanthroline as a colorless glassy product (1.89 g, 60%). ¹H NMR (CDCl₃, 200 MHz): δ = 0.96 (t, *J* = 6 Hz, 3H), 1.40 (m, 2H), 1.63 (m, 2H), 2.71 (t, *J* = 6 Hz, 2H), 7.36 (d, *J* = 8 Hz, 2H), 7.65 (dd, *J* = 4 and 8 Hz, 1H), 7.80 (AB, *J* = 9 Hz, 2H), 8.10 (d, *J* = 8 Hz, 1H), 8.29 (m, 4H), 9.26 (dd, *J* = 4 and 1 Hz, 1H); C₂₂H₂₀N₂ (312.41): calcd C 84.58, H 6.45, N 8.97; found C 84.31, H 6.66, N 8.90.

Preparation of 2,9-Bis(4-*n*-Butylphenyl)-1,10-phenanthroline (5). A 1.6 M *n*-BuLi solution (6.9 mL, 11.04 mmol) was added by syringe at room temperature to an argon-flushed, stirred solution of 4-bromo-*n*-butylbenzene (2.34 g, 11.00 mmol) in dry Et₂O (40 mL). After 1.5 h, the resulting yellow solution was added under argon to a degassed solution of 2-(4-*n*-butylphenyl)-1,10-phenanthroline (1.80 g, 5.76 mmol) in dry Et₂O (100 mL) at room temperature. The resulting dark red mixture was stirred for 5 h and then hydrolyzed with water. The bright yellow ether layer was decanted and the aqueous layer extracted with CH₂Cl₂ (3×). The combined organic layers were thereafter rearomatized by addition of MnO₂ (30 g), dried (MgSO₄), and filtered; the filtrate was then evaporated to dryness. Column chromatography on SiO₂ (CH₂Cl₂) yielded **5** as a colorless glassy product (1.95 g, 76%). ¹H NMR (CDCl₃, 200 MHz): δ = 0.99 (t, *J* = 6 Hz, 6H), 1.44 (m, 4H), 1.70 (m, 4H), 2.74 (t, *J* = 6 Hz, 4H), 7.42 (d, *J* = 8 Hz, 4H), 7.79 (s, 2H), 8.14 (d, *J* = 8 Hz, 2H), 8.30 (d, *J* = 8 Hz, 2H), 8.39 (d, *J* = 8 Hz, 4H); ¹³C NMR (CDCl₃, 50 MHz): δ = 13.96, 22.33, 33.49, 35.48, 119.67, 125.73, 127.53, 127.65, 128.87, 136.70, 136.91, 144.38, 146.02, 156.73; C₃₂H₃₂N₂ (444.62): calcd C 86.45, H 7.25, N 6.30; found C 86.31, H 7.42, N 6.36.

General Procedure for the Preparation of the Copper(I) complexes. A solution of Cu(CH₃CN)₄·BF₄ (0.6 equiv) in CH₃CN was added under an argon atmosphere at room temperature to a stirred, degassed solution of the phenanthroline derivative (1 equiv) in CH₂Cl₂. The mixtures turned dark red instantaneously, indicating the formation of the complexes. After 1 h, the solvents were evaporated. The resulting complexes were purified by column chromatography on Al₂O₃ (CH₂Cl₂/5% MeOH) followed by recrystallization from CH₂Cl₂/pentane [(2)₂Cu·BF₄, (4)₂Cu·BF₄, and (5)₂Cu·BF₄] or CH₂Cl₂/MeOH [(3)₂Cu·BF₄]. The copper(I) complexes were thus obtained in 80–95% yields.

(2)₂Cu·BF₄: ¹H NMR (CDCl₃, 200 MHz): δ = 0.56 (t, *J* = 6 Hz, 12H), 0.58–0.90 (m, 24H), 1.39 (m, 8H), 2.71 (t, *J* = 6 Hz, 8H), 7.80 (d, *J* = 8 Hz, 4H), 8.08 (s, 4H), 8.58 (d, *J* = 8 Hz, 4H); ¹³C NMR (CDCl₃, 50 MHz): δ = 13.61, 22.00, 28.85, 29.60, 30.76, 40.23, 124.61, 126.15, 127.74, 137.57, 142.97, 161.51; C₄₈H₆₄N₄CuBF₄ (847.41): calcd C 68.03, H 7.61; found C 67.68, H 7.60.

(3)₂Cu·BF₄: ¹H NMR (acetone-*d*₆, 200 MHz): δ = 0.80 (m, 16H), 1.48 (m, 8H), 2.82 (t, *J* = 6 Hz, 8H), 3.05 (m, 8H), 8.05 (d, *J* = 8 Hz, 4H), 8.26 (s, 4H), 8.80 (d, *J* = 8 Hz, 4H); ¹³C NMR (acetone-*d*₆, 50 MHz): δ = 24.97, 26.54, 32.84, 41.09, 61.81, 61.93, 126.13, 127.12, 128.93, 138.55, 138.75, 162.83; IR (CH₂Cl₂): 3077 cm^{-1} (O–H); C₄₄H₅₈N₄O₄CuBF₄ (857.32): calcd C 61.64, H 6.82; found C 61.55, H 6.67.

(4)₂Cu·BF₄: ¹H NMR (CD₂Cl₂, 200 MHz): δ = 0.67 (m, 8H), 0.93 (m, 8H), 1.37 (m, 8H), 1.94 (s, 12H), 2.73 (t, *J* = 6 Hz, 8H), 3.57 (t, *J* = 6 Hz, 8H), 7.85 (d, *J* = 8 Hz, 4H), 8.11 (s, 4H), 8.62 (d, *J* = 8 Hz, 4H); ¹³C NMR (CD₂Cl₂, 50 MHz): δ = 20.69, 25.35, 27.53, 29.17, 39.98, 63.43, 124.92, 126.21, 127.75, 137.82, 142.81, 161.10, 170.67; IR (CH₂Cl₂): 1732 cm^{-1} (C=O); C₅₂H₆₄N₄O₈CuBF₄ (1023.45): calcd C 61.03, H 6.30; found C 61.06, H 6.57.

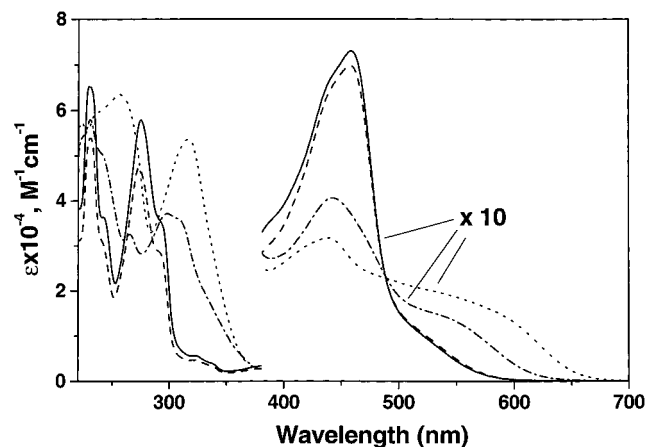


Figure 1. Absorption spectra of $[\text{Cu}(\mathbf{1})_2]^+$ (dash line), $[\text{Cu}(\mathbf{2})_2]^+$ (full line), $[\text{Cu}(\mathbf{5})_2]^+$ (dot line), and $[\text{Cu}(\mathbf{6})_2]^+$ (dash-dot line) in CH_2Cl_2 solution at 298 K. Over the 380–700 nm region a multiplying factor of 10 is applied.

($\mathbf{5}$) $\text{Cu}\cdot\text{BF}_4$: ^1H NMR (CD_2Cl_2 , 200 MHz): $\delta = 0.89$ (t, $J = 6$ Hz, 12H), 1.17 (m, 16H), 2.18 (t, $J = 6$ Hz, 8H), 6.34 (d, $J = 8$ Hz, 8H), 7.36 (d, $J = 8$ Hz, 8H), 7.83 (d, $J = 8$ Hz, 8.09 (s, 4H), 8.50 (d, $J = 8$ Hz, 4H); ^{13}C NMR (CD_2Cl_2 , 50 MHz): $\delta = 13.85, 22.07, 33.24, 34.77, 124.35, 126.27, 126.95, 127.62, 127.93, 135.99, 137.04, 143.16, 144.06, 156.41$.

Spectroscopic Investigations. The solvents used for spectroscopic investigations were CH_2Cl_2 and CH_3OH (Carlo Erba, spectrofluorimetric grade). The samples were placed in fluorimetric 1-cm path cuvettes and, when necessary, purged from oxygen by bubbling argon or by using freeze–thaw–pump cycles. Absorption spectra were recorded with a Perkin-Elmer $\lambda 5$ spectrophotometer. Uncorrected emission spectra were obtained with a Spex Fluorolog II spectrofluorimeter (continuous Xe lamp, 150 W), equipped with a Hamamatsu R-928 photomultiplier tube. The corrected spectra were obtained via a calibration curve determined by means of a 45-W quartz-halogen tungsten filament lamp (Optronic Laboratories) calibrated in the range 400–1800 nm. The calibration curve is flat (no correction required) between 400 and 550 nm and then increases steeply giving a correction factor of 7, 25, and 210 at 700, 800, and 850 nm, respectively. Fluorescence quantum yields in neat CH_2Cl_2 solvent were obtained from spectra on an energy scale (cm^{-1}) according to the approach described by Demas and Crosby⁴⁶ and using air-equilibrated $[\text{Os}(\text{phen})_3]^{2+}$ in acetonitrile ($\Phi_{\text{em}} = 0.005$)⁴⁷ as standard. For steady-state and time-resolved luminescence experiments at 77 K we employed a 1:1 (v/v) mixture of CH_2Cl_2 and MeOH, that was found to yield sufficiently transparent glasses. In this case, the samples were placed in Pyrex capillary tubes (2 mm diameter) immersed in liquid nitrogen contained in a homemade quartz dewar. Temperature-dependent measurements in the range 300–96 K were also performed on $\text{CH}_2\text{Cl}_2/\text{MeOH}$ samples deaerated by means of several freeze–thaw–pump cycles. Homemade 1-cm path quartz cells were employed which were placed in the modified holder of a liquid nitrogen Thor C600 cryostat. Emission lifetimes in the ns– μs time scale were determined with an IBH single-photon counting spectrometer equipped with a thyratron gated nitrogen lamp working in the range 4–40 kHz ($\lambda_{\text{exc}} = 337$ nm, 0.5 ns time resolution); the detector was a red-sensitive (185–850 nm) Hamamatsu R-3237–01 photomultiplier. The uncertainties are ± 2 nm, $\pm 20\%$, and $\pm 5\%$, for emission maxima, emission intensities and quantum yields, and excited-state lifetimes, respectively.

Results and Discussion

Electronic Absorption Spectra. The absorption spectra of $[\text{Cu}(\mathbf{1})_2]^+$, $[\text{Cu}(\mathbf{2})_2]^+$, $[\text{Cu}(\mathbf{5})_2]^+$, and $[\text{Cu}(\mathbf{6})_2]^+$ are displayed in Figure 1; the spectra of $[\text{Cu}(\mathbf{3})_2]^+$ and $[\text{Cu}(\mathbf{4})_2]^+$ are not shown

(46) Demas, J. N.; Crosby, G. A. *J. Phys. Chem.* **1971**, *75*, 991.

(47) Kober, E. M.; Caspar, J. V.; Lumpkin, R. S.; Meyer, T. J. *J. Phys. Chem.* **1986**, *90*, 3722.

Table 1. Photophysical Properties at 298 K in CH_2Cl_2 Solution

	$\lambda_{\text{max}}(\text{em})^a$ (nm)	$10^4\Phi_{\text{em}}^b$	τ^c (ns)	$10^{-3}k_r^d$ (s^{-1})	$10^{-6}k_{nr}^e$ (s^{-1})	$10^{-6}k_q[\text{O}_2]^f$ (s^{-1})
$[\text{Cu}(\mathbf{1})_2]^+$	674 (748)	3 (4)	56 (72)	5.6	13.8	4.0
$[\text{Cu}(\mathbf{2})_2]^+$	660 (724)	7 (10)	98 (132)	7.6	7.6	2.6
$[\text{Cu}(\mathbf{3})_2]^+$	660 (724)	6 (8)	84 (107)	7.5	9.3	2.6
$[\text{Cu}(\mathbf{4})_2]^+$	658 (718)	8 (11)	107 (152)	7.2	6.6	2.8
$[\text{Cu}(\mathbf{5})_2]^+$	692 (718)	8 (12)	139 (224)	5.4	4.4	2.7
$[\text{Cu}(\mathbf{6})_2]^+g$	686 (745)	3 (4)	107 (130)	2.8	7.7	1.7

^a Emission maxima from uncorrected and, in brackets, corrected spectra. ^b Emission quantum yields in air-equilibrated and, in brackets, air-free solutions. ^c Excited-state lifetimes in air-equilibrated and, in brackets, air-free solutions. ^d Radiative decay rate constants in air-free solution. ^e Nonradiative decay rate constants in air-free solution. ^f Stern–Volmer rate constants for the quenching of the luminescent excited state by O_2 , calculated from lifetimes in air-free and air-equilibrated solutions. ^g From ref 34.

since they are very similar, if not identical, to those of $[\text{Cu}(\mathbf{1})_2]^+$ and $[\text{Cu}(\mathbf{2})_2]^+$.

The spectral shapes of complexes of 2,9-dialkylphenanthrolines **1–4** are substantially the same both in the UV and in the vis spectral region, regardless the length of the alkyl chain. The spectrum of $[\text{Cu}(\mathbf{5})_2]^+$, instead, is quite peculiar. In the UV region, where the ligand-centered ($\pi-\pi^*$) transitions of the phenanthroline ligands are dominant, the difference recorded for $[\text{Cu}(\mathbf{5})_2]^+$ is attributable to the presence of the phenyl fragment conjugated to the phenanthroline unit. As far as the vis region is concerned, both electronic and structural factors (phenyl/phenanthroline π -stacking interactions, leading to flattening distortions)^{22,48} can explain the pattern of the MLCT bands of the phenylphenanthroline-type complex $[\text{Cu}(\mathbf{5})_2]^+$, as already discussed.¹ The pronounced shoulder around 550 nm is commonly taken as a fingerprint for 2,9-aryl substitution of the phenanthroline ring, when the other positions remain free.^{24,28}

As is typical for complexes of dialkylphenanthrolines,¹ the complexes of ligands **1–4** exhibit a low-intensity absorption feature above 500 nm that is accompanied by a much sharper and intense absorption band around 460 nm (ϵ_{max} ca. $7000 \text{ M}^{-1} \text{ cm}^{-1}$), to be compared to the weaker band of $[\text{Cu}(\mathbf{5})_2]^+$ ($\epsilon_{\text{max}} = 3200 \text{ M}^{-1} \text{ cm}^{-1}$, 438 nm).⁴⁹

It is important to notice that, in the visible spectral region (Figure 1), the absorption spectrum of the complex of the asymmetric ligand **6** exhibits intermediate intensities of the features around 450 and 550 nm, if compared to the spectra of the symmetric alkyl- or phenyl-phenanthroline complexes. The isosbestic point at 488 nm ($\epsilon = 2300 \text{ M}^{-1} \text{ cm}^{-1}$) for the spectra of Figure 1 might be accidental; however, it could also indicate some subtle regularity in intensity band variations on passing from alkyl to phenyl substituents.

Emission Spectra at 298 K. The luminescence data at 298 K in CH_2Cl_2 , along with some related quantities, are collected in Table 1. All of the complexes show a luminescence band that can be attributed to the deactivation from MLCT excited states^{1,2} (Figure 2).

The recorded spectra require severe instrumental correction in the region of interest (550–850 nm, see Experimental

(48) Cesario, M.; Dietrich-Buchecker, C. O.; Guilhem, J.; Pascard, C.; Sauvage, J. P. *J. Chem. Soc., Chem. Commun.* **1985**, 244.

(49) Dietrich-Buchecker, C. O.; Marnot, P. A.; Sauvage, J. P.; Kirchoff, J. R.; McMillin, D. R. *J. Chem. Soc., Chem. Commun.* **1983**, 513.

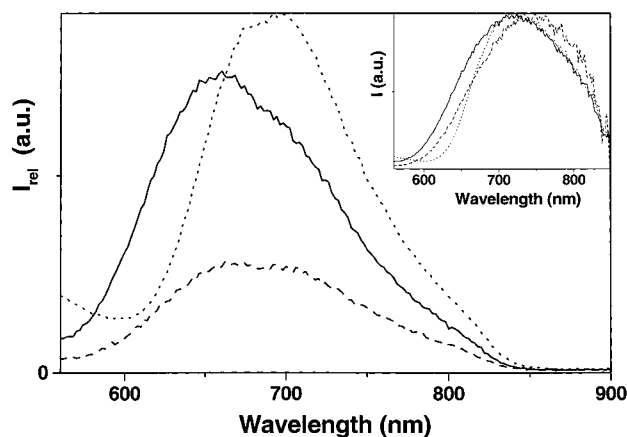


Figure 2. Uncorrected luminescence spectra of $[\text{Cu}(\mathbf{1})_2]^+$ (dash line), $[\text{Cu}(\mathbf{2})_2]^+$ (full line), and $[\text{Cu}(\mathbf{5})_2]^+$ (dot line) in CH_2Cl_2 solution at 298 K upon excitation at 440 nm. The optical density of all samples is identical (0.240); thus, the spectra are comparable in terms of relative emission intensity. The spectra corrected for the photomultiplier response (normalized) are reported in the inset.

Section), so that the emission maxima are remarkably shifted to longer wavelength upon correction (Table 1, Figure 2). The uncorrected luminescence spectra of $[\text{Cu}(\mathbf{1})_2]^+$, $[\text{Cu}(\mathbf{2})_2]^+$, and $[\text{Cu}(\mathbf{5})_2]^+$ (Figure 2) look somewhat different. However, upon correction, the spectral shapes tend to uniform, and the only remarkable difference is the 20 nm red-shift of the $[\text{Cu}(\mathbf{1})_2]^+$ maximum, compared to that of the other two compounds. The shapes of the luminescence spectra of $[\text{Cu}(\mathbf{2})_2]^+$, $[\text{Cu}(\mathbf{3})_2]^+$, and $[\text{Cu}(\mathbf{4})_2]^+$ are quite similar to each other, in line with the absorption behavior.

The better luminescence performance of the complexes of **2–5** relative to $[\text{Cu}(\mathbf{1})_2]^+$ can be rationalized on the basis of the protection exerted toward the copper ion by the cumbersome substituents in the 2 and 9 positions of phenanthroline. These residues contrast the excited-state distortion of the complex and tend to prevent the formation of pentacoordinated exciplexes (with solvent molecules or counterions), that funnel the deactivation of the potentially luminescent $[\text{Cu}(\text{NN})_2]^+$ MLCT levels via non radiative paths.^{17,50} Among the investigated complexes, both in air-equilibrated and in oxygen-free solution, $[\text{Cu}(\mathbf{5})_2]^+$ exhibits the highest emission quantum yield and the longest lifetime at room temperature, the former being comparable to those of $[\text{Cu}(\mathbf{2})_2]^+$ and $[\text{Cu}(\mathbf{4})_2]^+$. The radiative deactivation rate constant ($k_r = \Phi_{\text{em}}/\tau$) of $[\text{Cu}(\mathbf{5})_2]^+$ (Table 1) is the smallest of the series, but this is largely compensated by the value of the nonradiative rate constant ($k_{\text{nr}} = 1/\tau$), that turns out to be the smallest as well.⁵¹ As a result, $[\text{Cu}(\mathbf{5})_2]^+$ is the best room-temperature luminophore of the series. A comparison between $[\text{Cu}(\mathbf{2})_2]^+$ and $[\text{Cu}(\mathbf{3})_2]^+$ is interesting since the substituents on the phenanthroline ligands are alkyl chains of similar length, but with different terminal groups (Chart 1). The lower emission quantum yield and shorter lifetime displayed by $[\text{Cu}(\mathbf{3})_2]^+$ can be due to some internal exciplex dynamic quenching promoted by the terminal basic OH groups, possibly interacting with the copper ion in the excited state. A similar, more effective,

(50) McMillin, D. R.; Kirchhoff, J. R.; Goodwin, K. V. *Coord. Chem. Rev.* **1985**, *64*, 83.

(51) Since the luminescence of Cu(I)–phenanthrolines is attributable to two excited states in thermal equilibrium (a higher-lying singlet MLCT level and a lower-lying related triplet, see text) the calculated values of the radiative and nonradiative rate constants are not strictly referred to one specific excited state; therefore, they can be better defined as observed rates. However, at least at room temperature, the luminescence is mainly attributable to the singlet excited level and, as a first approximation, the observed rate constants can be related to it.

Table 2. Photophysical Properties in $\text{CH}_2\text{Cl}_2/\text{MeOH}$ (1:1, v/v) Glass at 77 K, Unless Otherwise Noted

	$\lambda_{\text{max}}(\text{unc.})^a$ (nm)	intensity	τ (μs)	$\Delta E_{298\text{K}-77\text{K}}^b$ (cm^{-1})
$[\text{Cu}(\mathbf{1})_2]^+$	706 (738)	weak	0.82	−180
$[\text{Cu}(\mathbf{2})_2]^+$	646 (676)	strong	2.40	−980
$[\text{Cu}(\mathbf{3})_2]^+$	644 (678)	strong	2.36	−940
$[\text{Cu}(\mathbf{4})_2]^+$	640 (672)	strong	3.13	−950
$[\text{Cu}(\mathbf{5})_2]^+$	736 (772)	faint	<i>c</i>	+980
$[\text{Cu}(\mathbf{6})_2]^+^d$	730 (760)	weak	~ 0.5	−260

^a Emission maxima from uncorrected and, in brackets, corrected spectra. ^b Calculated from emission bands maxima of the corrected spectra. Negative sign means blue-shift, positive sign means red-shift. ^c Not measured due to signal weakness. ^d In CH_2Cl_2 matrix, from ref 34.

intramolecular quenching of $[\text{Cu}(\text{NN})_2]^+$ MLCT excited states was proposed for 2,9-disubstituted phenanthrolines with appended toluidine residues.⁴⁴

Emission Spectra at 77 K. Luminescence data in $\text{CH}_2\text{Cl}_2/\text{MeOH}$ glass at 77 K, are collected in Table 2. Under these conditions all of the complexes are luminescent, but the trend of the intensity is quite variable along the series.

It has been reported several times that the luminescence intensity of $[\text{Cu}(\text{NN})_2]^+$ systems decreases when the temperature is decreased. To explain this unusual behavior, a model involving two MLCT excited states in thermal equilibrium, that is, a singlet (¹MLCT) and a related triplet (³MLCT) have been proposed (“two-state model”) by McMillin.^{16,19} The energy gap between these states has been sometimes reported to be 1000–2000 cm^{-1} ^{19,52} and, at room temperature, population of the upper-lying ¹MLCT level is achieved to some extent. By temperature decrease, such thermal activation is depressed until only the lowest ³MLCT level is significantly populated. The radiative rate constant of the ³MLCT level is much smaller than that of the ¹MLCT one; thus, in the former case nonradiative processes are comparably more important. As a result, deactivation of the ³MLCT state gives a much weaker luminescence than ¹MLCT, thus leading to the unconventional low-emission intensity at low temperature.^{19,34,35,52} Furthermore, under the latter conditions, the emission band is usually found to be red shifted (emission from ³MLCT) in comparison to that in fluid room-temperature solution (emission from higher-lying ¹MLCT).^{19,34,35,52}

By inspecting the emission data at *only* two temperature values (298 and 77 K, Tables 1 and 2 respectively) one could conclude that the above two-level model is unable to explain all of our experimental results since, for instance, $[\text{Cu}(\mathbf{2})_2]^+$ (Figure 3), $[\text{Cu}(\mathbf{3})_2]^+$, and $[\text{Cu}(\mathbf{4})_2]^+$ (Table 2) are very strong emitters at 77 K.

Noticeably their bright orange luminescence is observable also by naked eye and, though a quantitative measure in a rigid matrix is difficult, we can roughly estimate that the emission quantum yields of the complexes of **2–4** are at least 100 times higher than those of $[\text{Cu}(\mathbf{1})_2]^+$ and $[\text{Cu}(\mathbf{5})_2]^+$. Another unexpected result is that, in passing from 298 to 77 K, complexes of alkylphenanthrolines **1–4** display emission *blue*-shifting (very small in the case of **1**), while for the complex of arylphenanthroline **5** the spectrum is *red*-shifted (Table 2).

(52) Parker, W. L.; Crosby, G. A. *J. Phys. Chem.* **1989**, *93*, 5692.

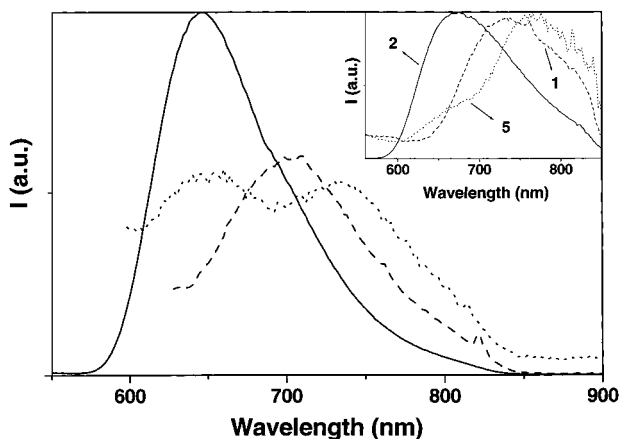


Figure 3. Uncorrected luminescence spectra of $[\text{Cu}(\mathbf{1})_2]^+$ (dash line), $[\text{Cu}(\mathbf{2})_2]^+$ (full line), and $[\text{Cu}(\mathbf{5})_2]^+$ (dot line) in a $\text{CH}_2\text{Cl}_2/\text{MeOH}$ 1:1 (v/v) glass at 77 K upon excitation at 440 nm. The spectra corrected for the photomultiplier response are reported in the inset. The experimental emission intensity of $[\text{Cu}(\mathbf{2})_2]^+$ is by far the strongest (see text), and the intensity on the ordinate scale is arbitrary, to allow a comparison. The 77 K spectrum of $[\text{Cu}(\mathbf{5})_2]^+$ exhibits two maxima separated by about 2000 cm^{-1} . This value is likely to correspond to a vibronic progression since the difference between the two emitting excited states in this complex (McMillin's model) is found to be 660 cm^{-1} (see text).

From the above temperature dependent trends in luminescence intensity and emission spectral shift (when only two temperature values are examined, i.e., 298 and 77 K), one could conclude that the two-level model can be fully applied in the case of $[\text{Cu}(\mathbf{5})_2]^+$ and $[\text{Cu}(\mathbf{6})_2]^+$ (emission intensity decrease and spectral red-shift upon cooling), can reasonably hold in the case of $[\text{Cu}(\mathbf{1})_2]^+$ (emission intensity decrease and slight blue-shift), but can hardly explain the behavior of $[\text{Cu}(\mathbf{2})_2]^+$, $[\text{Cu}(\mathbf{3})_2]^+$, and $[\text{Cu}(\mathbf{4})_2]^+$ (emission intensity increase and marked blue shift). In an attempt to rationalize these conflicting experimental findings we decided to make detailed investigations on the temperature dependence of the luminescence properties of $[\text{Cu}(\mathbf{2})_2]^+$ (taken as a representative of the series $[\text{Cu}(\mathbf{2})_2]^+$, $[\text{Cu}(\mathbf{3})_2]^+$, and $[\text{Cu}(\mathbf{4})_2]^+$) and $[\text{Cu}(\mathbf{5})_2]^+$.

Temperature Dependence of the Luminescence Spectra.

For $[\text{Cu}(\mathbf{2})_2]^+$ and $[\text{Cu}(\mathbf{5})_2]^+$ in deaerated $\text{CH}_2\text{Cl}_2/\text{MeOH}$ 1:1 (v/v), we have recorded the luminescence spectra (Figures 4 and 5) and the lifetimes in the temperature interval 300–96 K; in the range 130–110 K the solvent passes from fluid to frozen state.

Figure 6 shows the trend of the luminescence band maxima (top panel), and the relative emission intensities (bottom panel) as a function of temperature.

Close inspection of the results summarized in Figures 4–6 allows the following points to be listed.

(i) For the aryl-phenanthroline complex $[\text{Cu}(\mathbf{5})_2]^+$, on passing from 300 to 96 K, the emission maximum is bathochromically shifted (Figure 6a), thus pointing to an increased stabilization of the luminescent level. This is accompanied by a steady decrease in luminescence intensity (Figure 6b), in line with the behavior of many $[\text{Cu}(\text{NN})_2]^+$ complexes reported throughout the years.³⁵ As mentioned above, this is interpreted in terms of the two-state model with the lowest-lying level being poorly luminescent.^{19,34,35,52}

(ii) For the alkyl-phenanthroline compounds $[\text{Cu}(\mathbf{2})_2]^+$, a more complex behavior is found on lowering the temperature. Here, stabilization of the emitting level is maximized in the interval 120–150 K (Figure 6a) but further lowering of temperature till

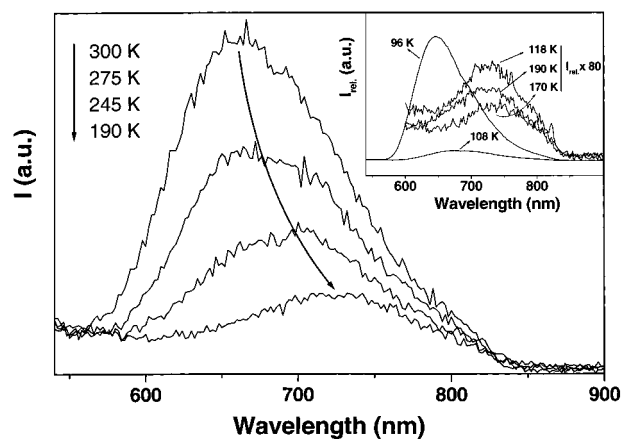


Figure 4. Uncorrected luminescence spectra of $[\text{Cu}(\mathbf{2})_2]^+$ in a $\text{CH}_2\text{Cl}_2/\text{MeOH}$ 1:1 (v/v) at different temperatures down to 190 K. In the inset the trend at temperatures below 190 K is shown; the very weak spectra at 190, 170, and 118 K are multiplied by a factor of 80 to allow a comparison with the much more intense signals at lower temperatures (108 and 96 K). λ_{exc} is always kept at 456 nm.

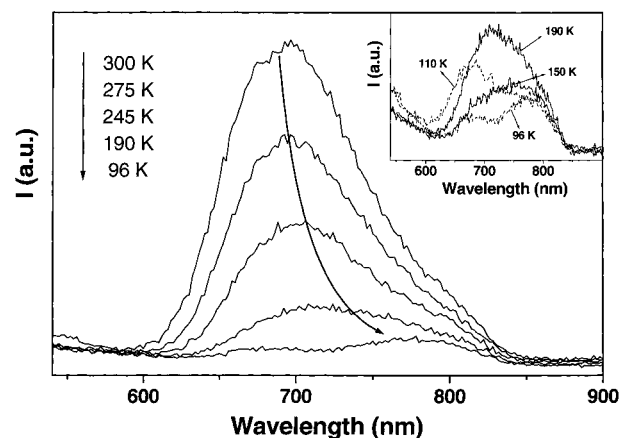


Figure 5. Uncorrected luminescence spectra of $[\text{Cu}(\mathbf{5})_2]^+$ in a $\text{CH}_2\text{Cl}_2/\text{MeOH}$ 1:1 (v/v) at different temperatures down to 96 K; $\lambda_{\text{exc}} = 440\text{ nm}$. In the inset the trend between 190 and 96 K is emphasized.

96 K (frozen solvent) causes a steady destabilization of the luminescent level by ca. 2000 cm^{-1} (ca. 1000 cm^{-1} by comparing data at 298 and 77 K only, Table 2). A similar behavior (in the frozen domain) has been frequently observed for complexes of the Ru(II)–polypyridine family in polar solvent and has been associated with the charge-transfer nature ($^3\text{MLCT}$) of the emitting levels;⁸ on the contrary, for $[\text{Cu}(\text{NN})_2]^+$ complexes, no extended temperature-dependent investigations have been reported to date. For $[\text{Cu}(\mathbf{2})_2]^+$, it is thus observed an “oscillating” trend in the luminescence pattern as a function of temperature (Figures 4 and 6): an intensity decrease and spectral red-shift is found in the range 300–120 K then a dramatic intensity increase and blue-shift is recorded by further cooling. This latter finding is particularly interesting because to date Cu(I)–bisphenanthrolines have been commonly considered poor luminophores in low-temperature rigid matrices.

Below, we discuss the nature of the excited levels involved in the emission processes and suggest a rationale to explain the different excited-state dynamics of $[\text{Cu}(\mathbf{2})_2]^+$ and $[\text{Cu}(\mathbf{5})_2]^+$.

Temperature Dependence of the Excited-State Lifetimes.

For both $[\text{Cu}(\mathbf{2})_2]^+$ and $[\text{Cu}(\mathbf{5})_2]^+$ these investigations were carried out with a single photon counting spectrometer and by using cutoff filters in order to include the full emission region. In all cases the emission decays occurred as single exponentials.

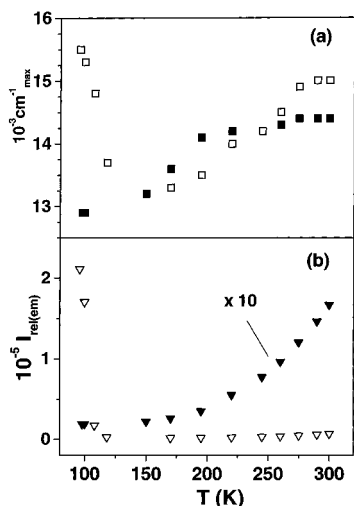


Figure 6. Temperature dependence in the 300–96 K range of (a) luminescence band maxima (cm^{-1} , from uncorrected spectra) and (b) relative emission intensities of $[\text{Cu}(\mathbf{2})_2]^+$ ($\lambda_{\text{exc}} = 456 \text{ nm}$, open points) and $[\text{Cu}(\mathbf{5})_2]^+$ ($\lambda_{\text{exc}} = 440 \text{ nm}$, solid points) in $\text{CH}_2\text{Cl}_2/\text{MeOH}$ 1:1 (v/v). The emission intensity data of $[\text{Cu}(\mathbf{5})_2]^+$ (solid triangles) are multiplied by a factor of 10 for the sake of clarity.

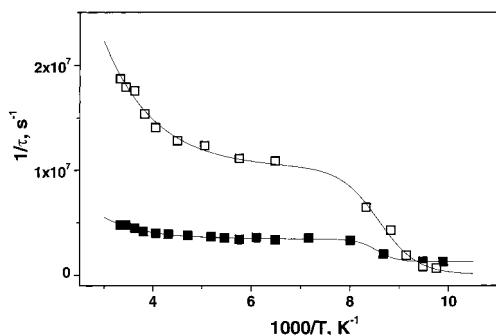


Figure 7. Temperature dependence of the luminescence lifetimes in the 300–96 K range for $[\text{Cu}(\mathbf{2})_2]^+$ (open squares) and $[\text{Cu}(\mathbf{5})_2]^+$ (solid squares) in $\text{CH}_2\text{Cl}_2/\text{MeOH}$ 1:1 (v/v); $\lambda_{\text{exc}} = 337 \text{ nm}$.

According to the two-state model, we have analyzed the data with an Arrhenius-type approach;^{42,43} therefore, the reciprocal of the lifetime ($1/\tau$) was plotted against the reciprocal of temperature ($1000/T$), Figure 7.

As one can see from the Figure, the $1/\tau$ versus $1/T$ trend is qualitatively similar for both complexes and the experimental data points can be fitted with the following equations in both cases.

$$1/\tau = A \exp\left(-\frac{\Delta E}{RT}\right) + k'_0 \quad (1a)$$

$$k'_0 = k_0 + \frac{B}{1 + \exp[C(1/T - 1/T_g)]} \quad (1b)$$

(1a) is an Arrhenius-type equation, where a term taking care of the glass-to-fluid transition region is added (k'_0 , eq 1b).^{42,43} In eq 1a, A and ΔE are, respectively, the preexponential factor and the energy barrier for thermal redistribution of the excited species between the levels of the two-state model. k'_0 (eq 1b) includes a low-temperature limiting rate constant, k_0 (that comprises the radiative and nonradiative contributions at 96 K), whereas B accounts for effects occurring around the glass-to-fluid transition temperature (T_g). Within this empirical description and given that the luminescence lifetime of the examined complexes is governed by nonradiative processes (i.e. $\tau \approx k_{\text{nr}}^{-1}$),

Table 3. Kinetic Parameters for Excited State Decay^a

	A (s^{-1})	ΔE (cm^{-1})	B (s^{-1})	k_0 (s^{-1})
$[\text{Cu}(\mathbf{2})_2]^+$	2.1×10^8	800	1.0×10^7	5.9×10^5
$[\text{Cu}(\mathbf{5})_2]^+$	6.8×10^7	660	2.1×10^6	1.3×10^6

^a In $\text{CH}_2\text{Cl}_2/\text{MeOH}$ 1:1 (v/v); from fitting of eqs 1 of the text to the experimental points of Figure 7; T_g was evaluated $117 \pm 5 \text{ K}$.

B represents the decrease of nonradiative rate constant observed on passing from fluid to frozen solvent. In the examined cases, T_g occurred in the interval 110–130 K, with the analysis providing $T_g = 117 \pm 5 \text{ K}$. Table 3 collects parameters obtained from the least-squares nonlinear fitting analysis of the data points displayed in Figure 7.

According to the results of this analysis, some issues can be highlighted.

(i) For both $[\text{Cu}(\mathbf{2})_2]^+$ and $[\text{Cu}(\mathbf{5})_2]^+$, the luminescence lifetime increases monotonically on passing from room temperature to 96 K (frozen solvent), Figure 7. According to the two-state equilibrium model for the lowest MLCT excited states of $[\text{Cu}(\text{NN})_2]^+$, use of eq 1 provided $\Delta E = 800$ and 660 cm^{-1} for, respectively, $[\text{Cu}(\mathbf{2})_2]^+$ and $[\text{Cu}(\mathbf{5})_2]^+$ (Table 3); this corresponds to the energy gap separating the two luminescent levels.

As for the nature of the two states (see above) it has been suggested that the higher-lying one is a singlet ($^1\text{MLCT}$) and the lower-lying a triplet ($^3\text{MLCT}$);¹⁹ this can explain the increase of the excited state lifetime accompanied by the bathochromic emission shift, upon temperature decrease. In our case only the trend in temperature dependence of the lifetimes is “conventional”; instead, for $[\text{Cu}(\mathbf{2})_2]^+$, the frozen state of the solvent causes a highly efficient population of the higher-lying emitting level, since the (very intense) emission is *hypsochromically* shifted. Interestingly, at 96 K the measured lifetime of $[\text{Cu}(\mathbf{2})_2]^+$ is 1510 ns, that is, twice the value of $[\text{Cu}(\mathbf{5})_2]^+$ (780 ns).

(ii) For both $[\text{Cu}(\mathbf{2})_2]^+$ and $[\text{Cu}(\mathbf{5})_2]^+$, the lifetime undergoes a stepwise change in the glass-to-fluid transition region, 100–130 K, see plot of Figure 7. This behavior is typical of CT levels of molecules embedded in polar solvents and is related to the fact that in frozen media these levels are destabilized because of the lack of solvent relaxation.^{42,43} In our case the solvent dielectric constants are 8.9 and 32.7 for CH_2Cl_2 and MeOH respectively, so the 1:1 mixture can be regarded as a solvent of intermediate polarity. The influence of the solvent is clearly larger for $[\text{Cu}(\mathbf{2})_2]^+$ than for $[\text{Cu}(\mathbf{5})_2]^+$ since the B parameter, that describes the jump observed in the plots of Figure 7, is 1.0×10^7 and $2.1 \times 10^6 \text{ s}^{-1}$, respectively (Table 3). This suggests that for $[\text{Cu}(\mathbf{2})_2]^+$ the luminescence might be associated with excited states bearing more CT character than for the latter case. In other words, according to a simplified picture, the (metal) promoted electron spreads over the LUMO of the ligand, so that the average distance of the electron from the metal center is larger in **2** than in **5**.²⁰ Therefore, the dipole vector associated with the CT state is expected to be larger in the case of the $[(\mathbf{2})\text{Cu}^{\text{II}}(\mathbf{2}^-)]^+$ excited complex than for $[(\mathbf{5})\text{Cu}^{\text{II}}(\mathbf{5}^-)]^+$. Another explanation for the different glass-to-fluid transition in the two compounds has to do with the blocking of structural distortions in frozen solvent, as is pointed out below.

Influence of the Ground- and Excited-States Geometries on the Photophysical Properties. Absorption spectra. The ideal ground-state geometry for $[\text{Cu}(\text{NN})_2]^+$ complexes corresponds to a quasi-tetrahedral D_{2d} symmetry.^{1–3} Upon light absorption, the population of the lowest-lying MLCT excited

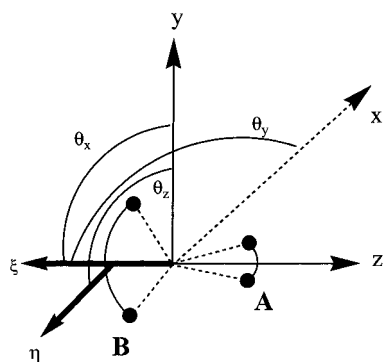


Figure 8. Relative orientation of the two ligand planes (A and B) and of the reference θ_z , θ_x , and θ_y angles. yz is the plane of the sheet; the black circles represent the N phenanthroline atoms; the Cu ion coincides with the origin of the reference axes; z is the direction bisecting both N–Cu–N triangles; the vector ξ lies on the B plane, the vector η is perpendicular to it (see ref 15).

states leads to geometrical distortions, whose extent depends on specific structural factors related to the substitution patterns of the phenanthroline ligand. Figure 8 provides an illustration of the parameters that describe the distortions from an ideal tetrahedral geometry.¹⁵

Of great importance are the θ_z and θ_x angles that define the “flattening” and “rocking” distortions of the phenanthroline ligands with respect to each other. In practice, combinations of various types of distortions are likely to occur.

The absorption spectra of $[\text{Cu}(\mathbf{2})_2]^+$, $[\text{Cu}(\mathbf{5})_2]^+$ and $[\text{Cu}(\mathbf{6})_2]^+$ (Figure 1) provide a nice illustration of the control exerted by the molecular geometry over the optical properties. We notice first that for $[\text{Cu}(\mathbf{2})_2]^+$, whose geometry is assumed to be close to D_{2d} , only one intense vis absorption band is present ($\lambda_{\text{max}} = 458 \text{ nm}$, $\epsilon = 7300 \text{ M}^{-1} \text{ cm}^{-1}$). According to McMillin, such absorption band can be associated to a MLCT z -polarized transition along the C_2 axis bisecting the Cu–NN angle (Figure 8).¹⁶ This involves one orbital of the $e_{d(xz,yz)}$ metal set and one (π^* LUMO) orbital from the ligand system.

The presence of one or two phenyl residues on the chelating phenanthroline, causes a marked change in the spectral shape (Figure 1). This is a consequence of interligand (phenyl/phenanthroline) π -stacking interactions that favor distortions from the tetrahedral geometry.^{22,53} Interestingly, the integrated areas Y of the absorption profiles of $[\text{Cu}(\mathbf{2})_2]^+$, $[\text{Cu}(\mathbf{5})_2]^+$, and $[\text{Cu}(\mathbf{6})_2]^+$ in the 25000–14300 cm^{-1} range (400–700 nm, Figure 1) are 3200, 3000, and 2500 $\text{M}^{-1} \text{ cm}^{-2}$ respectively. The fact that such values are reasonably comparable may suggest that the strong transition associated with the absorption band of $[\text{Cu}(\mathbf{2})_2]^+$ actually undergoes a splitting into two main contributions (two bands around 450 and 550 nm, respectively) in the case of $[\text{Cu}(\mathbf{5})_2]^+$ and of $[\text{Cu}(\mathbf{6})_2]^+$, as a consequence of symmetry lowering. At odds with what was hypothesized by Shinozaki and Kaizu,⁵⁴ small deviations of the θ_z and θ_x angles (5 – 15°) are sufficient for yielding a neat dual band behavior, as recently reported by Karpishin.²⁸ Thus, if deviations from the D_{2d} arrangement are not so large to induce scrambling of the metal orbital energy layout, it might well be that the two observed low-energy bands of Figure 1, with maxima around 450 and 550 nm, correspond to transitions from metal orbitals to the LUMO+1 and LUMO levels of the ligands. In Figure 9, an illustration for the $d_{yz} \rightarrow \psi_{\text{LUMO}+1}$ and $d_{yz} \rightarrow \chi_{\text{LUMO}}$ z -allowed

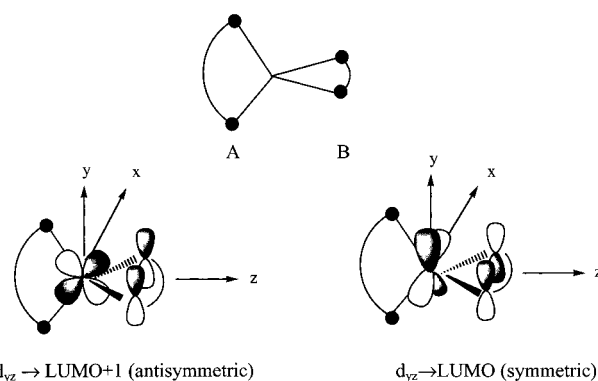


Figure 9. Orbital interaction schemes under local C_{2v} symmetry between the Cu ion (at the center of the reference system) and ligand A.

transitions is provided, according to a very simplified description of the orbital interactions under a local C_{2v} symmetry.¹⁶

For phen, the LUMO/LUMO+1 energy gap is evaluated 0.8 eV by using standard extended Huckel molecular orbital (EHMO) calculations, to be compared with an experimental energy difference of the two vis absorption features in $[\text{Cu}(\mathbf{5})_2]^+$ and $[\text{Cu}(\mathbf{6})_2]^+$ of ca. 0.6 eV.

Emission Spectra and Lifetimes. The correlation between geometric and luminescence properties in $[\text{Cu}(\text{NN})_2]^+$ complexes is more difficult to discuss, since several factors should be taken into account.¹⁶ They include (i) the effect of specific distortions due to the d^9 excited-state electronic configuration at the metal center, (ii) the fact that two very close emitting MLCT levels can be involved, and (iii) the possible role of spin–orbit coupling in determining the symmetry (i.e., the forbidden character) of the lowest-lying cluster of MLCT states. At any rate, in practice, the luminescent MLCT excited states of $[\text{Cu}(\text{NN})_2]^+$ complexes are usually reported to be stabilized by decreasing temperatures; this may result in very low (if any) luminescence intensity, as it happens for our $[\text{Cu}(\mathbf{5})_2]^+$ complex. Two effects could account for this uncommon spectroscopic behavior: (i) the typical decrease of emission yield when the energy of an emitting level is decreased (energy-gap law),^{39–41} (ii) the intermolecular quenching of $[\text{Cu}(\text{NN})_2]^+$ excited states via formation of exciplexes with donating solvents in fluid media.¹⁷ The stepwise $1/\tau$ vs $1/T$ behavior around 117 K, Figure 7, indicates that on passing from fluid to rigid medium the nonradiative deactivation steps are depressed to a different extent for $[\text{Cu}(\mathbf{2})_2]^+$ and $[\text{Cu}(\mathbf{5})_2]^+$, $B = 1.0 \times 10^7$ and $2.1 \times 10^6 \text{ s}^{-1}$, respectively. In the case of the diphenyl-phenanthroline ligand ($[\text{Cu}(\mathbf{5})_2]^+$), comparison of the plots of Figures 4 and 7 suggests a minor role for “energy gap law” effect, since the change of state of the solvent negligibly affects the emission energy position. On this basis, the observed change in nonradiative rate for $[\text{Cu}(\mathbf{5})_2]^+$ ($B = 2.1 \times 10^6 \text{ s}^{-1}$) is likely due to inhibition of exciplex quenching owing to a reduced mobility of the partners in the frozen solvent.

On the contrary, for $[\text{Cu}(\mathbf{2})_2]^+$, the luminescent level is destabilized by about 2000 cm^{-1} on freezing the solvent, and a very intense luminescence is observed. We interpret this behavior as a consequence of the blocking of the complex geometry to the ground state arrangement in the rigid matrix. In this case, substantial “energy-gap law” effects are expected. We found $B = 1.0 \times 10^7 \text{ s}^{-1}$ for $[\text{Cu}(\mathbf{2})_2]^+$, and a comparison with the B value obtained for $[\text{Cu}(\mathbf{5})_2]^+$ (see above) may suggest that in the former only 20% of B is related to quenching by the solvent, the remaining effect being ascribable to changes in excited-state energy level (energy gap law). The luminescence

(53) Meyer, M.; Albrecht-Gary, A. M.; Dietrich-Buchecker, C. O.; Sauvage, J. P. *Inorg. Chem.* **1999**, *38*, 2279.

(54) Shinozaki, K.; Kaizu, Y. *Bull. Chem. Soc. Jpn.* **1994**, *67*, 2435.

behavior of $[\text{Cu}(\mathbf{3})_2]^+$ and $[\text{Cu}(\mathbf{4})_2]^+$, that is identical to that of $[\text{Cu}(\mathbf{2})_2]^+$, can be rationalized with the same arguments.

The prominence of structural over electronic factors, to explain the observed “anomalous” luminescence behavior at low temperatures for $[\text{Cu}(\mathbf{2})_2]^+$, $[\text{Cu}(\mathbf{3})_2]^+$, and $[\text{Cu}(\mathbf{4})_2]^+$, is confirmed by the luminescence properties of $[\text{Cu}(\mathbf{1})_2]^+$. Such complex, though of alkylphenanthroline-type, has been known to be a poor emitter at low temperatures since a long time.¹⁹ The small methyl residues are likely not able to prevent some minimal excited-state distortion even in rigid matrix, just enough to yield weak luminescence.

Conclusions

A relevant issue for to the design of Cu(I)–phenanthroline complexes exhibiting improved luminescence properties (i.e. high emission intensity and long excited-state lifetimes) is concerned with a full understanding of the structural and electronic properties of the luminescent MLCT excited states. The long-term holding of the so-called two-level model has provided guidelines in this respect.¹⁶ According to this model, the low-temperature emission is foreseen very weak. However, we show here that at low temperature, when the solvent is rigid, some complexes may exhibit enhanced luminescence. Our findings are not in contrast with the two-state model but, on the contrary, bring further evidence to support its validity. The picture that stems from this investigation shows that two emitting MLCT excited states are always present *as long as excited-state distortions can occur*. At room temperature, despite strong differences in the absorption spectra, the luminescence properties are similar for all complexes, the variability of emission performances being predominantly ascribable to “external” factors such as bimolecular exciplex quenching.¹⁷ When the temperature is decreased, yet remaining in a *fluid* domain, the emission band is decreased in intensity and shifted to lower energy for *all* complexes, in agreement with the two-state model. Then, when the solvent is transformed into a rigid matrix (below 120 K in our cases) the trends differentiate. The “regular” behavior is still followed in the case of $[\text{Cu}(\mathbf{5})_2]^+$ (where distortions are intrinsically present due to intramolecular

π -stacking interactions, see absorption spectrum) and $[\text{Cu}(\mathbf{1})_2]^+$ (where distortions can still occur in the excited state even below 120 K, see above). On the contrary, long alkyl chains on the phenanthroline ligands prevent both type of distortions. As a result, the lower-lying poorly emitting MLCT level is not apparently involved, and the observed strong luminescence arises from the (sole) upper lying MLCT state.

We believe that this work provides a relevant breakthrough toward the optimization of the luminescence performances of Cu(I)–phenanthrolines,^{1–3} since it is suggested that *both* bulkiness⁴⁴ and alkyl-nature of the ligands are necessary features to observe luminescence in frozen media. Our observations, coupled with those recently reported by the groups of McMillin²⁴ and Karpishin²⁹ can give clear guidelines for the synthesis of highly luminescent and long-lived complexes both in fluid solution and in rigid matrix. In the latter case the Cu(I) complex is not necessarily embedded in low-temperature glasses but can be a room-temperature solid sample;⁵⁵ indeed, it has been recently demonstrated that even pristine $[\text{Cu}(\text{phen})_2]^+$ is weakly luminescent in the solid state.²⁵ It is thus conceivable that, for instance, complexes bearing long alkyl chains in the 2,9 and methyl residues in the 3,8 positions of the phenanthroline ring can be ideal $[\text{Cu}(\text{NN})_2]^+$ luminophores, displaying strong luminescence both in fluid and in rigid media. Further, the availability of simple Cu(I)–phenanthrolines displaying long-lived and strongly luminescent excited states in rigid (solid) matrix would open new perspectives in terms of practical applications (e.g. photovoltaic technology and chemical sensing), thus increasing the competition toward $[\text{Ru}(\text{bpy})_3]^{2+}$ -type complexes.¹

Acknowledgment. This work was supported by the Italian CNR and French CNRS. We thank Mr. M. Minghetti for technical assistance. Financial support from the European Union (TMR Network ERBFMRX CT 980226) is gratefully acknowledged.

JA0043439

(55) Eggleston, M. K.; Fanwick, P. E.; Pallenberg, A. J.; McMillin, D. R. *Inorg. Chem.* **1997**, *36*, 4007.